Boom, echo, pulse, flow

(Open version)

Tim Riffe*[1], Kieron Barclay[1], Christina Bohk-Ewald[1], and Sebastian Klüsener[2]

[1]Max Planck Institute for Demographic Research
[2]Bundesinstitut für Bevölkerungsforschung

December 1, 2018

Abstract

Human population renewal starts with births. Since births can happen at any time in the year and over a wide range of ages, demographers typically imagine the birth series as a continuous flow. Taking this construct literally, we visualize the Swedish birth series as a flow. A long birth series allows us to juxtapose the children born in a particular year with the children that they in turn had over the course of their lives, yielding a crude notion of cohort replacement. Macro patterns in generational growth define the meandering path of the flow, while temporal booms and busts echo through the flow with the regularity of a pulse.

Keywords: Fertility, Population structure, Population momentum, Population renewal, Data visualization

1 Introduction

Usually demographers think of fertility as an age-regulated process. In any case it is bounded by menarche and menopause, both of which are anchored to age. These anchors may move, but not far or fast. And between these bounds, at least within acceptably homogeneous subpopulations, fertility patterns appear to conform to some regular schema. Since births can happen at any time throughout the year, and since demography usually deals in large numbers, it is common to imagine the birth flow as a continuous stream. This is so not only as a pragmatic assumption to allow for calculus, but it also gives us a heuristic understanding of fertility as a smoother of population structure (Arthur 1982). In the present exposition, we retreat from rates, the material of projections and stable theory, to the absolute number of babies born, the raw material of population renewal.

We aim to represent a historical view of Sweden's historical birth series in a single multilayered visualization. The birth series is rendered as a flow, in such a way as to be suggestive of novel analytic perspectives, and to invite newcomers and curious minds deeper into the discipline of demography. This image entails investment from the viewer, and this manuscript serves as a protracted legend and caption. Intellectual payoffs include a simultaneous sense of long term patterns of generational mixing and generational replacement, medium term baby booms and echos, and the short term shocks of population momentum. We challenge more experienced demographers to relate this image to the Lexis diagram, to imagine how the picture would change if fertility were indexed to fathers' age, or to reimagine this image of aggregates as an immense set of lineages.

Our Lexis time series of birth counts stretches from 1735 until 2016, and it is augmented by a projection of the completed fertility of cohorts through 2016, bringing the lastest year of birth to 2071. The temporal spread from the earliest mother cohort in our final data set (1687) to the latest offspring cohort (2071) is

*riffe@demogr.mpg.de

385 years. We describe our input data and adjustments to it briefly in Sec. 2, and in a detailed appendix, which serves as an annotation to the open code repository.

2 Data and methods

We use birth count data from Sweden in single-year bins by year of ocurrence and mother cohort, covering a total of 281 occurrence years from 1736 to 2016. Birth counts for years 1736 to 1750 are reconstructed from a variety of sources (Human Fertility Collection 2018, Human Mortality Database 2018, Statistika Centralbyrån 1969) using indirect methods (see App. A.1). Data for years 1751-1774 are derived via adjustment from HFC estimates and HMD exposures and birth totals (see App. A.2). Data for the period 1775 to 1890 come from Statistique Générale de la France (1907), which we have graduated (see App. A.3). The merged birth count series for years 1736 to 1890 is subject to a global adjustment to retain information on cohort size in patterns of cohort fertility (see App. A.4). Data for the years 1891 to 2016 is taken directly from the Human Fertility Database (2018) without further adjustment. To complete our picture, we project the fertility of cohorts whose fertility careers were still incomplete as of 2016 (1962-2016) through age 55 (see App. A.5). These steps are fully reproducible, and further details can be found in an open data and code repository.[1]

3 Age and cohort-structured birth count distributions

A picture of the births in a year is for demographers most instinctively broken down by the age of mothers who gave birth in that year, Fig. 1a, or by the year of birth of mothers Fig. 1b. These two distributions are essentially identical, but appear as mirror images if chronological time is enforced in x.

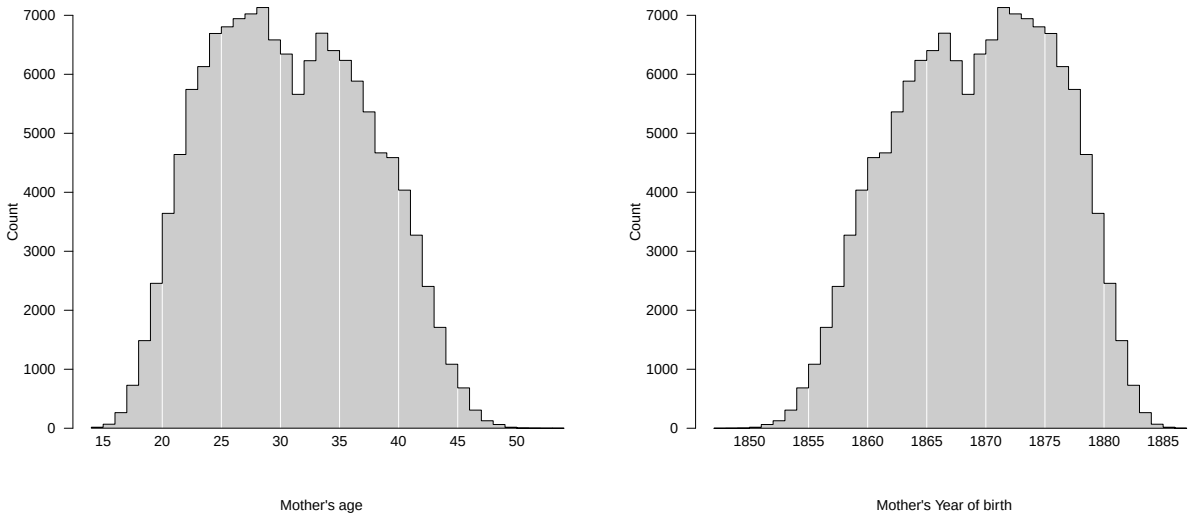

(a) Births in 1900 by age of mother

(b) Births in 1900 by year of birth of mother

Figure 1: Births in a year structured by mothers' age versus mothers' year of birth are a reflection over y and shift over x. Count distributions such as this may be jagged, even if the underlying rate distributions are smooth, due to population structure. The deficit around age 31 in 1a is due to a smaller number of potential mothers: the 1871 birth cohort was smaller than the surrounding cohorts.

[1] The reproducibility repository will either be `github` or `OSF`, to be determined.

If one disposes of a long-enough time series of births classified by mothers' year of birth, then one may further examine and break down the full reproductive career of the cohort of individuals born in a particular year, assuming no effects of migration. Since the childbearing of a cohort is spread over a synchronous span of ages and years, the classification by age (Fig. 2a) or year (Fig. 2b) yields identical and redundant distributions.

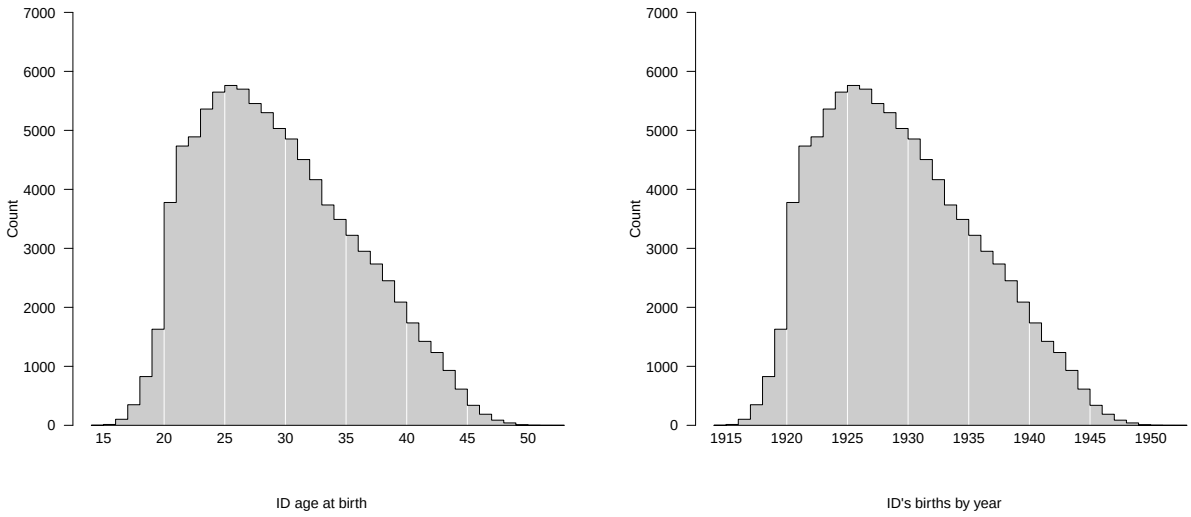

(a) Births from mothers born in 1900 by age of mother

(b) Births from mothers born in 1900 by year

Figure 2: Births of a cohort structured by mothers' age versus mothers' year of birth are a shift over x. The births over the life of a cohort more often resemble the smoothness of fertility rate schedules,

The births in a year are classified by mothers' cohort, i.e. cohort *origins* in Fig. 1b, whereas the births *from* a cohort are classified *to* time in Fig. 2b. The two distributions are different in kind, but relatable and both on a common scale. A fuller representation of their relationship would place them as two disjoint distributions on the same timeline, as in Fig 3.

The two distributions in Fig. 3 are related, and of comparable scale, but different in kind. The x coordinate of the left distribution is indexed to mothers' birth cohort, whereas the x coordinate of the right distribution is indexed to child cohort, occurrence year. In this way the respective x coordinates are two generations apart, relating to each other as grandmothers and grandchildren, where the *ego* generation is 1900. These are two quantities that we may wish to compare in various ways to get a better feel and understanding of the Swedish birth series.

For the case of our extended Swedish birth series, we have 281 such distribution pairs, making single-axis rendering impractical. An honest attempt might look like Fig. 4, where we reflect the Fig. 3 left distribution over y (**A**), keeping the Fig. 3 right-side distribution on top (**B**). These two distributions are linked by the year 1900, which of course overlaps with neither of them. In this representation, **A** and **B** are re-drawn for each possible ego year (1775-2016), and therefore imply a large sequential set of overlapping distributions. Each 20th distribution is highlighted, but despite attempts to make this graph legible, i) the high degree of overlapping and ii) the spatial dissociation of each **A** — **B** pair makes the intended comparison difficult over the series.

Fig. 4 produces at least two noteworthy artifacts that we may wish to preserve and clarify. 1) First order differences in the top series appear to cascade into the lower series— This highlights a small constituent of population momentum (Keyfitz 1971): larger cohorts tend to have more offspring than smaller neighboring cohorts and vice versa, sudden fertility rate changes notwithstanding. 2) The com-

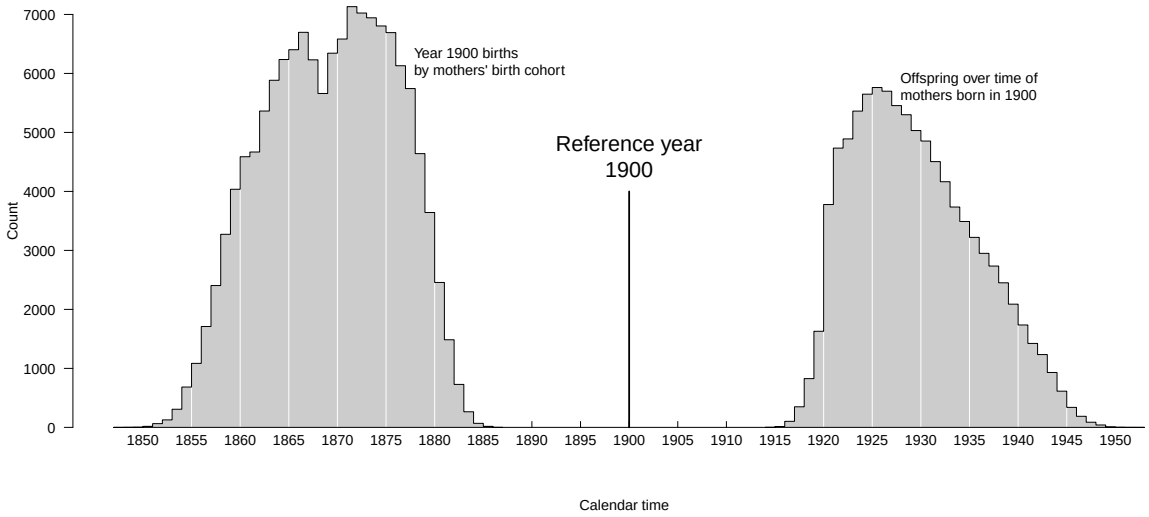

Figure 3: The cohort distribution of mothers who gave birth in 1900 and the births from mothers born in 1900 by year. These two distributions link three generations.

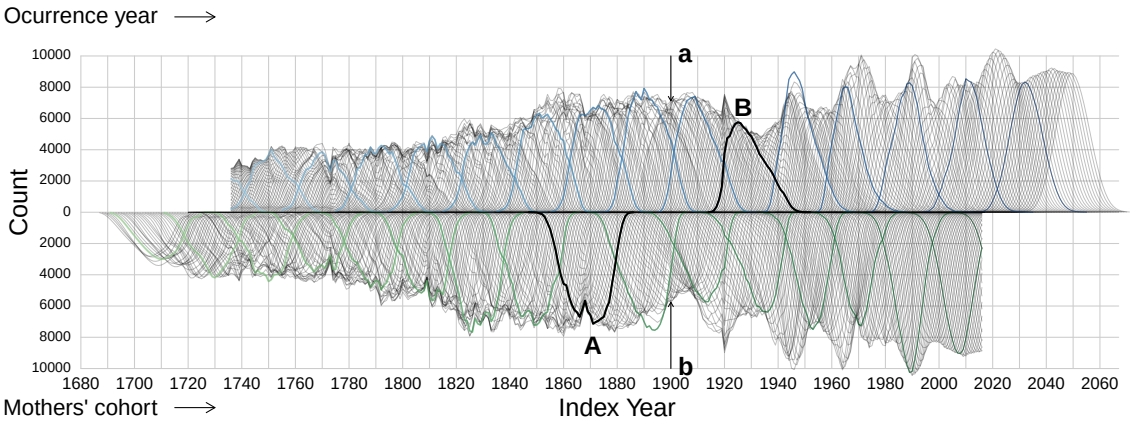

Figure 4: Two time series of birth count distributions. The top series is composed of offspring distributions of mother cohorts over time, indexed to occurrence years. The bottom series is composed of the offspring of a year indexed to mothers' birth cohorts. **B** is the offspring of mothers from the 1900 cohort indexed in x to occurrence year, and **A** are the births occurred in 1900 indexed in x to mothers' birth cohorts. The cross-section **a** gives **A** and the cross-section **b** gives **B**.

position of **A** in the bottom series is implied by the cross-section **a** of the top series, and the composition of **B** is implied by the cross-section **b**. This second observation merits further elaboration: The curve **A** is composed of all the births in 1900 indexed *back* to mothers' cohorts. Each point on the curve **A** comes from a different top-axis distribution as it crosses the year 1900 (and vice versa for the bottom). The cross-section of curves **a** is therefore a redundant encoding of the single highlighted curve **A**. The cross-section **b** is a redundant encoding of **B** in the same way. While **A** and **B** are disjoint, and difficult to relate, **a** and **b** share a single x coordinate, and so may lend themselves to comparison. The "problem" with the cross-sections **a** and **b** is that points from the corresponding distributions **A** and **B** are overlapped due to collapsation on a single x coordinate. It is basically impossible to work out what **A** (**B**) might look like if presented only with **a** (**b**) and its surroundings.

In this way the two distributions that we might wish to compare for a given ego year are already available at a like coordinate, but comparison is stifled by overplotting. If instead we stack the slices that are indecipherably overlapped in **a** (and likewise for **b**) we get something like that shown in Fig. 5, cumulative birth distributions.[2] Here the total bar length is proportional to the total cohort (offspring) size, and stacked bins reflect 5-year mother cohorts (occurrence years). From this representation it is clear that mothers born in the 20 years between 1860 and 1880 produced the bulk of the 1900 cohort (86%), which itself produced the majority of its offspring in the 20 years between 1920 and 1940 (90%). It is also quite visible that the 1900 cohort did not replace itself in a crude sense: 138,139 babies formed a cohort whose mothers gave birth to 95,379 babies over their lifecourse, a crude replacement of 69%. Other perspectives on reproduction that account for survival and attrition or growth of the mother cohort through migration would give a more optimistic assessment (Henry 1965). The key feature of Fig. 5 is that the two distributions that were disjoint in Fig. 3 and hard to pick out in Fig. 4 can now be associated at a common x coordinate. This virtue allows us to view the time series of Fig. 4 with greater clarity and hopefully reveal some macro properties of the history of Swedish natality.

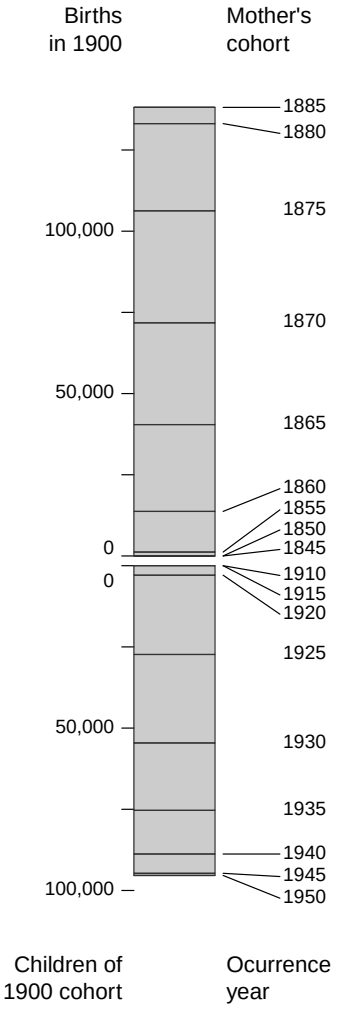

Figure 5: The 1900 cohort as a composite bar with its offspring reflected over y. The size of each bar stacked in the top composition is proportional to the area of its corresponding polygon in the left distribution of Fig. 3. The size of each bar stacked in the lower composition is proportional to the area of its corresponding polygon in the right distribution of Fig. 3.

4 Structuring the flow

Fig. 6 is a depiction of the exercise of Fig. 5, cohort bars on top reflected with offspring bars on the bottom. Equal bounded bins from Fig. 5 are joined into continuous regions. For the top region, filled polygons represent the births of mothers from quinquennial cohorts, spread over time. For the bottom region, filled polygons represent the mother-cohort origins (in x) of the births in quinquennial periods. Color darkness is proportional to the standard deviation of the birth distribution in each stacked polygon, with darker areas indicating more compact and lighter/brighter areas indicate wider distributions.

The meandering baseline of Fig. 6 is proportional to a smoothed time series of the crude cohort replacement rate (see App. A.6). We overlay a horizontal line to indicate periods of growth, replacement, and contraction. Periods where the meandering x-baseline is above this line (until ca 1865) indicate crude growth, and periods below the horizontal reference line (ca 1870 to 1930) indicate crude generation

[2] Young mothers are on top and older mothers on bottom for both distributions. It would also make sense to plot increasing (or decreasing) ages emanating out from the centerline in both directions.

[fold-out figure 4×a4 paper size at 100% in separate pdf, about here.]

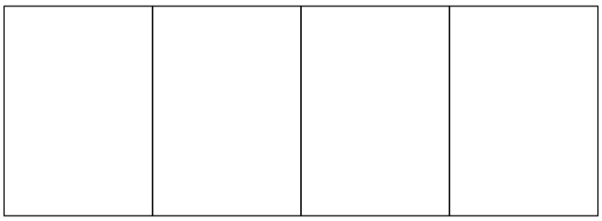

Figure 6: A time series of the same graphical construct as presented in Fig. 5. The x axis now meanders proportional to a smoothed time series of the crude cohort replacement ratio. Fill color darkness is proportional to the standard deviation of the time spread of each birth count distribution: Darker colors indicate more concentrated birth distributions and light colors indicate wider distributions. The birth series now appears as a flow, but reveals echoes in cohort and offspring size, a strong periodic series of booms and busts in recent decades, and a long term dampening of the crude replacement rate. Five generations of a female lineage is annotated atop to serve as a guide.

contraction. We call this crude replacement because the ratio takes no account of mortality or migration. The twentieth century was characterized by steady replacement by this measure.

To aid the viewer with interpretation, we overlay a lineage of five female generations, a subset of the ancestors and descendants of Alva Myrdal (born Reimer), who as much as anyone ought to remind us of the endogenous forces in the flow we depict.[3] Since the top and bottom portions of the graph are alternative depictions of the same data, each member of this lineage appears twice: once below her mother at the same x position, and once again on the top axis x-indexed to the year of birth and y indexed to mother cohort.

Several of the larger first differences in $B(t)$ (which cascade into $B(c)$) have likely explanations, in most cases owing to mortality shocks. A selection of these are labelled, and Utterström (1954) provides some complementary discussion. Medium-term deviations have often been characterized as cycles[TODO: ... to be continued]

5 Discussion

Several macro features come to the fore in this visualization. These are either known features of the Swedish birth series, or else merit further study.

Reproductivity Our Fig. 6 is broadly suggestive of the concept of population reproductivity. But the meandering baseline is proportional to the log of the ratio of offspring to mothers' "initial" cohort size, and for this reason it is not a sensitive measure of reproductivity: Death and migration stifle direct interpretation as such. There are other measures of reproductivity that take into account mortality (Kuczynski 1932), or both mortality and migration (Hyrenius 1951, Ortega and del Rey 2007, Preston and Wang 2007, Wilson et al. 2013, Ediev et al. 2014, inter alia), and which could therefore offer alternative meandering baselines. To take such indices at face value, the composite bins on the top and bottom axes would also change. Our visualization is nothing less or more than the Swedish birth flow. Indeed, the extended birth series we include as supplementary material could be used in part to calculate such sensitive indices.

Vibration, echoes, and cyclicity The birth series of Fig. 6 highlights the matched deviations in the size of cohorts and offspring. Neither these nor the larger scale varieties of cyclicity, such as those

[3] This descendancy continues, but births beyond Sissela are not depicted, and we were unable to ascertain the ancestors of Anna Lisa.

that appear through the 20th Century in Sweden are described at length herein. (Spanish flu recovery (Boberg-Fazlic et al. 2017))

Temporal mixture

References

W Brian Arthur. The ergodic theorems of demography: a simple proof. *Demography*, 19(4):439–445, 1982. doi: 10.2307/2061011.

Nina Boberg-Fazlic, Maryna Ivets, Martin Karlsson, and Therese Nilsson. Disease and Fertility: Evidence from the 1918 Influenza Pandemic in Sweden. IZA Discussion Papers 10834, Institute for the Study of Labor (IZA), June 2017. URL `https://ideas.repec.org/p/iza/izadps/dp10834.html`.

Christina Bohk-Ewald, Peng Li, and Mikko Myrskylä. Forecast accuracy hardly improves with method complexity when completing cohort fertility. *Proceedings of the National Academy of Sciences*, 115 (37):9187–9192, 2018.

Norman H Carrier and AM Farrag. The reduction of errors in census populations for statistically underdeveloped countries. *Population Studies*, 12(3):240–285, 1959. doi: 10.1080/00324728.1959.10405023.

Joop de Beer. A time series model for cohort data. *Journal of the American Statistical Association*, 80 (391):525–530, 1985. doi: 10.1080/01621459.1985.10478149.

Dalkhat Ediev, David Coleman, and Sergei Scherbov. New measures of population reproduction for an era of high migration. *Population, Space and Place*, 20(7):622–645, 2014.

O Grigorieva, A Jasilioniene, DA Jdanov, P Grigoriev, T Sobotka, K Zeman, and VM Shkolnikov. Methods protocol for the human fertility collection, 2015. URL `https://www.fertilitydata.org/docs/methods.pdf`.

Louis Henry. Réflexions sur les taux de reproduction. *Population (french edition)*, 20(1):53–76, 1965. doi: 10.2307/1526986.

Human Fertility Collection. Max Planck Institute for Demographic Research (Germany) and Vienna Institute of Demography (Austria). online, 2018. Available at www.fertilitydata.org (data downloaded on [Oct., 2018]).

Human Fertility Database. Max Planck Institute for Demographic Research (Germany) and Vienna Institute of Demography (Austria). online, 2018. Available at www.humanfertility.org (data downloaded on [Oct., 2018]).

Human Mortality Database. University of California, Berkeley (USA) and Max Planck Institute for Demographic Research (Germany), 2018. Available at www.mortality.org or www.humanmortality.de (data downloaded on Oct., 2018).

Hannes Hyrenius. Reproduction and replacement: A methodological study of swedish population changes during 200 years. *Population Studies*, 4(4):421–431, 1951.

Nathan Keyfitz. On the momentum of population growth. *Demography*, 8(1):71–80, 1971. doi: 10.2307/2060339.

R.R. Kuczynski. *Fertility and reproduction: methods of measuring the balance of births and deaths*. Falcon Press, 1932.

Juan Antonio Ortega and LA del Rey. Birth replacement ratios in europe: a new look at period replacement. [Unpublished] 2007. Presented at the Population Association of America 2007 Annual Meeting New York New York March 29-31 2007., 2007.

Marius D. Pascariu, Maciej J. Danko, Jonas Schoeley, and Silvia Rizzi. ungroup: An R package for efficient estimation of smooth distributions from coarsely binned data. *Journal of Open Source Software*, 3(29): 937, 2018. doi: 10.21105/joss.00937.

Samuel H Preston and Haidong Wang. Intrinsic growth rates and net reproduction rates in the presence of migration. *Population and Development Review*, 33(4):357–666, 2007.

Tim Riffe, Sean Fennell, and Jose Manuel Aburto. *DemoTools: Standardize, Evaluate, and Adjust Demographic Data*, 2018. URL `https://github.com/timriffe/DemoTools`. R package version 0.10.000.

Silvia Rizzi, Jutta Gampe, and Paul HC Eilers. Efficient estimation of smooth distributions from coarsely grouped data. *American journal of epidemiology*, 182(2):138–147, 2015. doi: 10.1093/aje/kwv020.

Henry S Shryock, Jacob S Siegel, and Elizabeth A Larmon. *The methods and materials of demography*. US Bureau of the Census, 1973.

Thomas Bond Sprague. Explanation of a new formula for interpolation. *Journal of the Institute of Actuaries*, 22(4):270–285, 1880. doi: 10.1017/S2046167400048242.

Statistika Centralbyrån. Historisk statistik för sverige. del 1, befolkning 1720-1967, 1969.

Statistique Générale de la France. *Statistique internationale du mouvement de la population daprès les registres détat civil: Résumé rétrospectif depuis lorigine des statistiques de létat civil jusquen 1905*. Imprimerie national, 1907.

Fil Lic Gustaf Utterström. Some population problems in pre-industrial sweden. *Scandinavian Economic History Review*, 2(2):103–165, 1954.

Chris Wilson, Tomáš Sobotka, Lee Williamson, and Paul Boyle. Migration and intergenerational replacement in europe. *Population and Development Review*, 39(1):131–157, 2013.

A Data sources and adjustments

Data presented here are from several different data sources, covering different time periods. These data originate in different APC bins, and some are derived using indirect methods or projection methods. The full list of sources is outlined in Tab. 1. Fig. 7 depicts the discrete Lexis bins of input data for the historical period before 1891. This appendix describes all steps taken to bring data into a standard format suitable for this study, and sections follow the order of the data processing steps undertaken. The data format required to build the figures in this manuscript consists in birth counts tabulated by single year of ocurrence and mother cohort, the PC Lexis shape (also denoted as 'VV' in HFD documents). Input data cover the years 1736 until 2016, with an oldest mother cohort of 1687. We complete the fertility of incomplete cohorts through 2016 up to age 55, bringing the latest year of occurence to 2071.

From	To	Data	Bins	Use	Source
1736	1750	birth counts	totals only	constraint	SCB
1751	1755	life tables	single ages 0-110	reverse survival	HMD
1751	each	population census	abridged ages	base for retrojection	HMD
1751	1774	ASFR	single-age, 5-year	infer births 1751-1774 & derive retrojection standard	HFC
1751	1774	population exposures	single-age and year	infer births	HMD
1751	1774	birth counts	totals only	constraint	HMD
1775	1890	birth counts	abridged ages	constraint	SGF
1891	2016	birth counts	single ages	as-is	HFD
1966	2016	ASFR	single ages	rate projection	HFD
2017	2071	Population projections	single ages	infer completed fertility	SCB

Table 1: Data sources

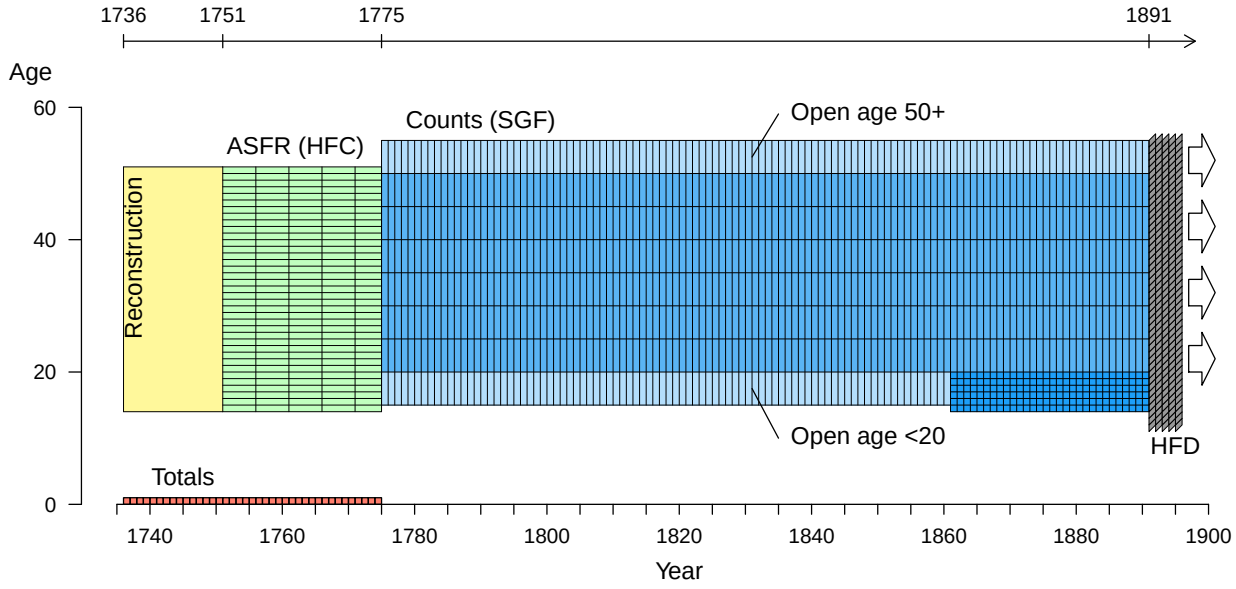

Figure 7: Lexis diagram depiction of fertility data sources and discrete Lexis bins for the period 1736-1890. Total counts are used as constraints for years 1736-1750, denoted with red boxes at age 0. The yellow box from 1736 to 1750 denotes the Lexis region over which birth counts are reconstructed using indirect techniques. The blue boxes from 1775 to 1890 indicate various age-period bins of birth counts. Light blue indicates lower and upper open age groups. Dark blue boxes in ages 14-19 from 1861-1890 indicate single year age-period bins. The HFD provides single-year period-cohort bins for birth counts starting in 1891 (gray).

A.1 Years 1736 - 1750

Estimating birth counts by single year of age for the 15 year period from 1736 to 1750 requires several steps of data processing and some strong assumptions. First, we reverse-survive females observed in the 1751 mid-year population census of Sweden, as extracted from the Human Mortality Database (2018) input database. Since this is a July 1 census, we take it as an acceptable proxy for exposure. The census originates in abridged ages $[0, 1, 3, 5, 10, 15 \ldots 90+]$. Examination of five year age groups suggests a underlying pattern age heaping, and for this reason we first smooth them using the so-called United Nations method (see Carrier and Farrag 1959) as implemented in the `DemoTools R` package (Riffe et al. 2018). We then graduate to single ages using the Sprague method (Sprague 1880, Shryock et al. 1973) as implemented in the `DemoTools R` package. This population is now the basis population to be reverse-survived through each single year until 1736, where we only make use of the fertile ages.

To reverse-survive, we use a standard survival curve defined as the age-specific arithmetic mean of the five single-age life table survival functions for the years 1751-1755 (Human Mortality Database 2018). The mid-year population count at age x, n years before the 1751 census $P(x, 1751 - n)$ is estimated as:

$$P(x, 1751 - n) = P(x + n, 1751) * \frac{\ell(x)}{\ell(x + n)} \qquad , \tag{1}$$

where $\ell(x)$ is the standard survival function described.

The next step is to derive a standard ASFR curve, $F(x)$. ASFR for the years 1751-1775 is given by the Human Fertility Collection (2018) in single ages and 5-year bins. If we rescale $F(x)$ in each 5-year period to sum to 1, one sees that there was very little shifting or shape changes in the period 1751-1774: each unity-scaled $F(x)$ curve is for practical purposes equivalent. We therefore take the standard fertility rate curve, $F^\star(x)$ to be their age-specific arithmetic mean, and we assume that it is valid for the year-range 1736 until 1750.

A first pass of unscaled birth counts at age x, t years before 1751 is taken as the product of estimated exposure and $F^\star(x)$.

$$\widehat{B}^\star(x, 1751 - n) = P(x, 1751 - n) \cdot F^\star(x) \tag{2}$$

The first pass of birth estimates implies a TFR of 1 in each year. Total births in each of these years $B(1751 - n)$ is known (Statistika Centralbyrån 1969, Tab. 27 & Tab. 28), so we derive our final estimate of age specific births, $\widehat{B}(x, 1751 - n)$ as:

$$\widehat{B}(x, 1751 - n) = \widehat{B}^\star(x, 1751 - n) \cdot \frac{B(1751 - n)}{\sum_{x=12}^{50} \widehat{B}^\star(x, 1751 - n)} \tag{3}$$

At this stage of processing, birth count estimates for the years 1736-1750 are given in single ages (AP Lexis squares). Further adjustments are carried out in common with later periods and described in the following sections.

A.2 Years 1751 - 1774

Estimating birth counts in single years and by single year of age for the 24 year period from 1751 to 1774 follows a similar logic, but it requires no retrojection. The Human Fertility Collection (2018) provides ASFR in single ages[4] in 5-year bins. The HMD provides exposure estimates $P(x, t)$ in single ages and years over this same period. A first-pass estimate of birth counts, $\widehat{B}(x, t)$ is given by:

$$\widehat{B}(x, t) = P(x, t) \cdot F(x, t') \qquad , \tag{4}$$

where t' denotes the 5-year bin in which t happens to fall. Year bins in the data are 5-years wide, and shifted up by 1, ergo 1751-1755, 1756-1760, and so forth. Following the convention of indexing to the lower bound, t' is defined as:

$$t' = 5\lfloor t/5 \rfloor + 1 \tag{5}$$

Births by single year of mothers' age are then rescaled to sum to the annual totals reported in the HMD:

$$B(x, t) = \widehat{B}(x, t) * \frac{B(t)}{\sum_{x=12}^{50} \widehat{B}(x, t)} \tag{6}$$

[4]This data was graduated by the HFC from 5×5 Lexis cells according to the HFC methods protocol (Grigorieva et al. 2015).

At this stage of processing, birth count estimates for the years 1751-1774 are given in single ages (AP Lexis squares). Further adjustments are carried out in common with later periods and described in the following sections.

A.3 Years 1775 - 1890

Birth counts for the 116 year period from 1775 to 1890 are available from Statistique Générale de la France (1907). These data are age-period classified, and given in a mixture of age classes, with a predominance 5-year age classes (especially for ages 20-50), but also sometimes single ages (especially for ages 15-19), and time-varying top and bottom open ages. We standardize these data in a few simple steps.

First, births of unknown maternal age were redistributed proportionally to the distribution of births of known maternal age. Second, counts are graduated to single ages using the graduation method proposed by Rizzi et al. (2015) and implemented in `R` in the package `ungroup` (Pascariu et al. 2018).

A.4 Years 1736 - 1890

At this stage of processing all birth counts for years 1736 until 1890 are in single age-period (AP) bins, and datasets covering the three periods are merged into a common dataset. Two further adjustments are performed, the first to move AP-bins into period-cohort (PC) bins. The second adjustment compensates for the smoothness of graduation methods so as to preserve the expected relationship between a cohort's size its total offspring size.

A.4.1 Adjustment to PC bins

Counts were shifted from AP Lexis bins into PC bins assuming that half of the births in each single age x bin go to the lower triangle of age $x+1$ and half to the upper triangle of the age-reached-during-the-year (PC) parallelogram at age x, as diagrammed in Fig. 8. At this point data are in a common format with the HFD data for the years 1891-2016, and these are merged into a single dataset.

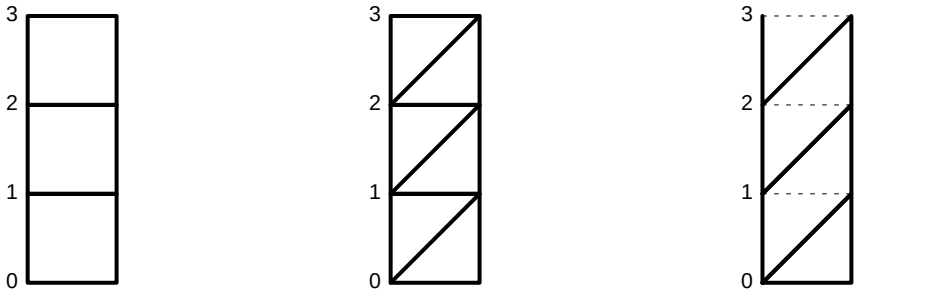

(a) AP square bins (b) Split evenly to triangles (c) Regroup to PC bins

Figure 8: The count regrouping procedure for years 1736 to 1890. Data are graduated to single ages (Fig. 8a), then split in half (Fig. 8b) and regrouped to period cohort (PC) bins (Fig. 8c).

A.4.2 Cohort size adjustment

At this stage of processing we have a harmonized dataset comprising a single series from 1736 until 2016 in consistent single-year PC bins. As such, one could produce the two time series represented in Fig. 6, albeit with a subtle artifact visible in Fig. 9. In area **A** of this figure, birth counts in age bins have been graduated using the previously mentioned pclm method, which has the usually-desired artifact of smoothness. For the affected range of years, mother cohorts are identified via the identity $C = P - A - 1$.[5] Since age patterns of counts are smooth, these sum in Lexis diagonals to a smooth time series of cohort total offspring, as seen in the profile of area **B** of the same figure. Area **C** of this figure delimits years 1875 until 1971, where both cohort and matched offspring sizes are directly observed,[6] and where fluctuations would appear to co-vary quite strongly. For the sake of a more sensible count graduation

[5] One subtracts 1 because data are in period-cohort bins.

[6] We estimate that the fertility of the 1971 cohort was over 99% complete as of 2016.

and for reasons of aesthetic continuity, we have opted to adjust the counts in area **B** to carry the pattern of fluctuation observed over cohort size from 1736 to 1890.

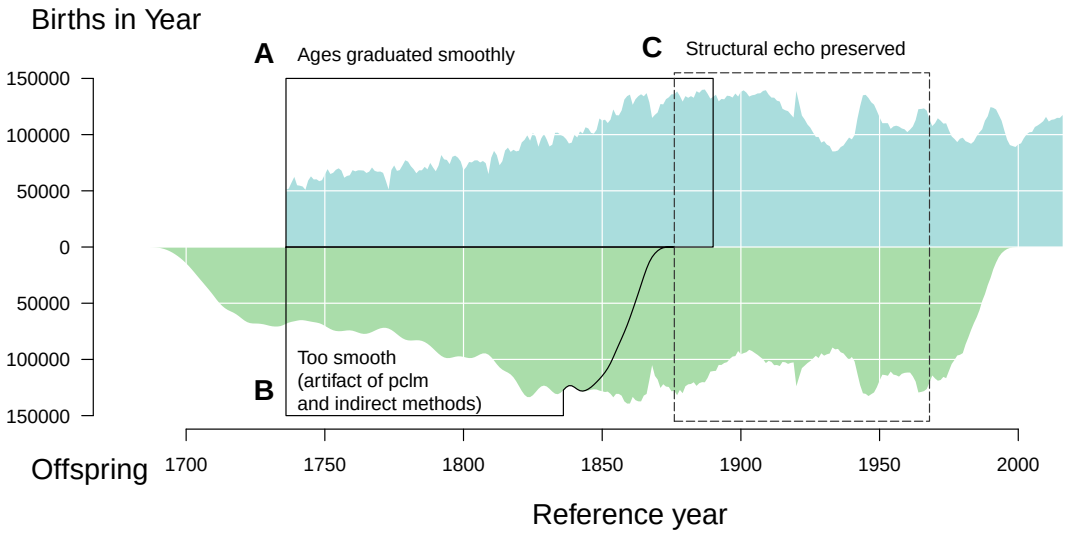

Figure 9: In reference years $\geq$ 1891 both births by year and cohort offspring are directly observed in single year bins, which means that the structural echo between total birth cohort and offspring size is preserved for reference years $\geq$ 1876 (**C**). Total per annum births in years $\leq$ 1890 (**A**) are presumed accurate, and so first differences of these are observed. Offspring from cohorts born in years $\leq$ 1876 (**B**) were partially (1836–1876) or entirely ($<$ 1836) born in years $\leq$ 1890, implying a smooth redistribution over single years of mother cohorts. We wish to adjust the births in **B** to recuperate the kind of structural echo in **C**.

This adjustment works by extracting the fluctuation pattern from **A** and transferring it to **B**. We do this by first smoothing the annual time series of total cohort size $B(t)$ according to some smoothness parameter, λ.[7] The ratio of $B(t)$ to the smoothed birth series $B(t)^s$ defines the multiplicative adjustment factor, $adj(t) = B(t)/B(t)^s$. Total offspring size $\mathbb{B}(c)$ is then adjusted as $\mathbb{B}(c)' = adj(t) * \mathbb{B}(c)$, for $c = t$. Counts in single ages are then rescaled to sum to the original totals in 5-year age groups, and counts for years $>$ 1890 are unaffected. The smoothing parameter is selected such that the linear relationship in fractional first differences $rd(B(t)) = \frac{B(t+1)-B(t)}{B(t)}$ between the annual birth series and adjusted offspring series $rd(\mathbb{B}(c)')$ for years 1736-1876 matches that for the reference years 1877-1971 as closely as possible. Specifically, we select λ so as to minimize the sum of the difference in slopes and residual standard deviations for the periods before and after 1891. Further clarifications about this adjustment, and code for diagnostic plots can be found in the annotated code repository. The end effect is to adjust the series to look like Fig. 10.

We adjusted in this way for the sake of a more nuanced time series of total offspring, but this approach may be used to good effect in graduating age-structured counts (births, deaths, populations) whenever time series are long enough to permit information on birth cohort size to propagate through the Lexis surface. These aspects are visible to some degree in the shaded polygons of Fig. 6 in years $<$ 1891.

[7] For the present case we've used a loess smoother, using the `R` function `loess()` with smoothing parameter $\lambda =$ `span`. It would be straightforward to swap this smoothing method out with a different one.

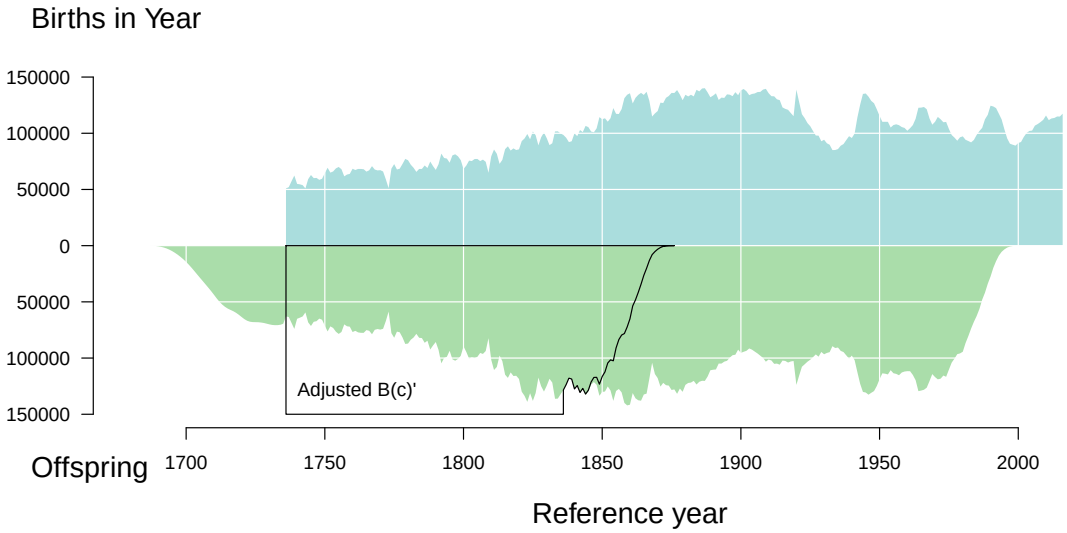

Figure 10: The adjusted birth series. Annual total births $B(t)$ on top axis and annual total offspring $\mathbb{B}(c)$ on bottom axis, with adjusted offspring counts $\mathbb{B}(c)'$ outlined.

A.5 Projected birth counts

[TODO: Christina should check this] Offspring counts by year of occurrence, $B(c,t)$ are only fully observed for years ≤ 1961. To complete the offspring reflection through the final reference year 2016, we have opted to project birth counts for cohorts whose fertility careers are incomplete (1962-2016). This is done by combining a projection of cohort fertility rates using the method proposed by de Beer (1985) with Sweden's official projection of population denominators to derive the implied birth counts by single year of age and time. The method used is parsimonious, and it performed very well in a comprehensive assessment of fertility forecast methods (Bohk-Ewald et al. 2018).

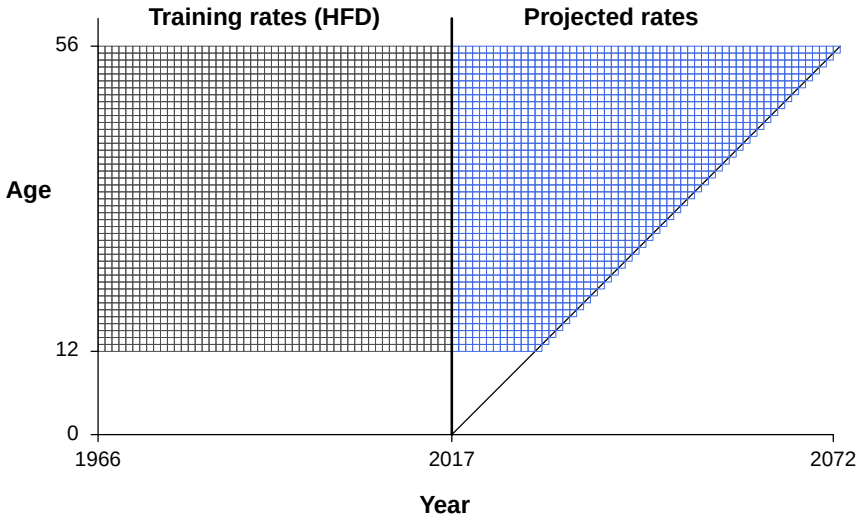

Figure 11: Diagram of the age and year-range of fertility rates used for model fitting and projection. We fit to 50 years of data (1966 until 2016), and project until the 2016 cohort (right bound of 2017) reaches age 55 in the year 2071 (right bound of 2072). The diagonal line delimits the data range after splitting to period-cohort bins.

Projected rates are then multiplied with SCB projected female population counts to derive implied births by age of mother. The projected birth counts are in single year age-period bins. These are then split to vertical parallelograms using the simple method described in Appendix A.4.1. The upward-slanting diagonal line in Fig. 11 marks the edge of the 2016 cohort fertility.

A.6 Meandering baseline

A peculiar feature of Fig. 6 is the meandering baseline, which replaces the standard straight-line x-axis. The baseline is derived from the crude cohort replacement rate $\mathbb{R}(c)$, defined as $\mathbb{R}(c) = \mathbb{B}(c = r)/B(t = r)$. This measure is not a replacement for the classic measure of net reproduction R_0, which differs in a few key ways: i) crude replacement is not sex-specific (our birth series is composed of boy and girl births combined), whereas R_0 is typically defined for females only. ii) while births arise from fertility rates over the life course, the number of potential mothers over the life course is not a mere function of mortality, but of migration as well, and the Swedish birth series will have been affected by heavy out-migration from 1850 until the Second World War, and some in-migration in more recent decades. Cohort R_0 is purged of population structure such as this (except to the extent that subgroups have differential vital rates), whereas $\mathbb{R}(c)$ is not, and for this reason we call it *crude*.

The series of $\mathbb{R}(c)$ is rather smooth without further treatment, save for 11 periodic breaks between 1970 and 1840, a period of rupture between 1865 and 1880, and another set of at least four breaks since the great depression in the 1930s. Rather than preserve these ruptures, we opt to smooth them out and instead capture long term trends in $\mathbb{R}(c)$ in the baseline, as seen in Fig. 12. Keeping the baseline meander smooth minimizes the visual penalty in assessing the variation in $\mathbb{B}(c)$ or $B(t)$ separately, and it enhances our ability to see the long term pattern. Specifically, we use use the `smooth.spline` from the `stats R` package, to smooth the $ln(\mathbb{R}(r))$ with smoothing parameter $\lambda = 0.00001$. The baseline that appears in Fig. 5 is the smooth prediction multiplied by 100,000.

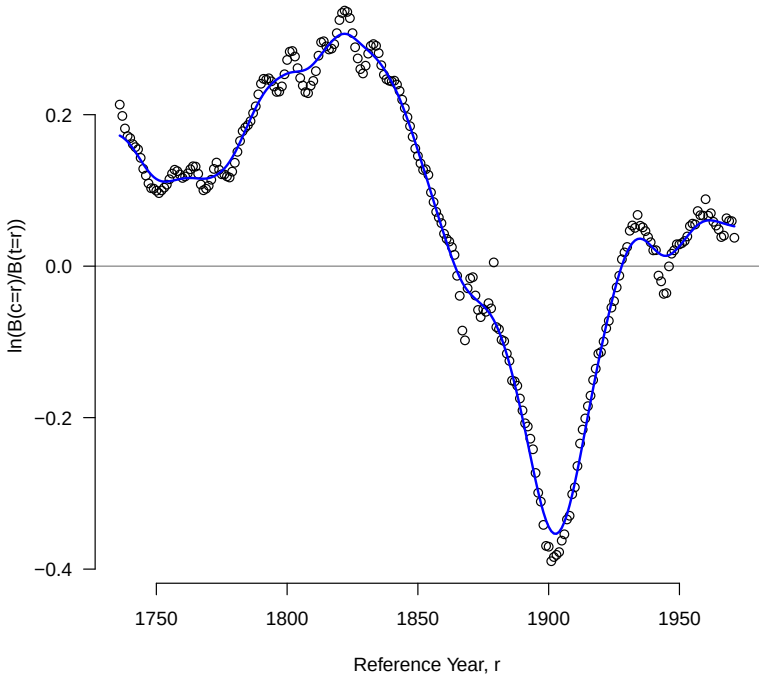

Figure 12: The time series of crude cohort replacement, $\mathbb{R}(c)$, and its smooth pattern (blue line) on which the Fig. 6 meandering baseline is based.